

## Detection of the microquasar V404 Cygni at $\gamma$ -rays revisited: only one flaring event in quiescence

YI XING<sup>1</sup> AND ZHONGXIANG WANG<sup>2,1</sup>

<sup>1</sup>Key Laboratory for Research in Galaxies and Cosmology, Shanghai Astronomical Observatory, Chinese Academy of Sciences, 80 Nandan Road, Shanghai 200030, China

<sup>2</sup>Department of Astronomy, Yunnan University, Kunming 650091, China

### ABSTRACT

The microquasar V404 Cygni (also known as GS 2023+338) was previously reported to have possible GeV  $\gamma$ -ray emission in two days during its 2015 outburst. In order to provide more detailed information at the high energy range for this black hole binary system, we conduct detailed analysis to the data obtained with the Large Area Telescope (LAT) onboard *the Fermi Gamma Ray Space Telescope (Fermi)*. Both LAT database and source catalog used are the latest. From the analysis, we can not confirm the previous detection. Instead, we find one possible detection ( $\sim 4\sigma$ ) of the source at the end of the outburst in the time period of 2015 Aug. 17–19, and one convincing detection ( $\simeq 7\sigma$ ) in 2016 Aug. 23–25. The latter shows that the  $\gamma$ -ray emission of the source is soft with photon index  $\Gamma \sim 2.9$ , mostly detected below  $\sim 1.3$  GeV with *Fermi* LAT. As  $\gamma$ -ray emission from microquasars is likely associated with their jet activity, we discuss the results by comparing with those well studied cases, namely Cyg X-3 and Cyg X-1. The detection establishes V404 Cygni as one of four microquasars with detectable  $\gamma$ -ray emission, and adds interesting features to the small group, or in a more general context to X-ray binaries with jets.

*Keywords:* stars: black holes — stars: individual (V404 Cygni) — gamma rays: stars — X-rays: binaries

### 1. INTRODUCTION

The X-ray binary V404 Cygni (or GS 2023+338) is a stellar-mass black hole system having a  $\sim 1 M_{\odot}$  low-mass companion star orbiting around a  $\sim 9 M_{\odot}$  black hole with an orbital period of 6.5 days (Casares et al. 1992; Casares & Charles 1994; Khargharia et al. 2010). The binary has a distance of 2.39 kpc (Miller-Jones et al. 2009). Long after a previous outburst in 1989 (Makino 1989), the source underwent another outburst in 2015. Both events triggered extensive observations at multi-frequencies. Particularly for the second outburst, which lasted from 2015 Jun. 15 (Barthelmy et al. 2015) to mid Aug. (Sivakoff et al. 2015; Plotkin et al. 2017), monitoring observations from radio to  $\gamma$ -rays were carried out. Different aspects of the binary, with particular attention to physical processes related to the black hole accretion (see, e.g., Belloni & Motta 2016), have been learned

from the observations (e.g., Rodriguez et al. 2015; Plotkin et al. 2017; Walton et al. 2017; Tetarenko et al. 2017; Maitra et al. 2017 and references therein). In addition at the end of 2015, a mini-outburst was seen from the source, which lasted approximately a month and exhibited similar features as those in the main 2015 outburst (see Muñoz-Darias et al. 2017 and references therein).

This black hole binary also belongs to the microquasar category (Mirabel & Rodríguez 1999), as jets associated with the black hole are believed to be present in its quiescence state (e.g., Gallo et al. 2005; Rana et al. 2016; Plotkin et al. 2019) and jet ejection was observed in the 2015 outburst (e.g., Walton et al. 2017; Tetarenko et al. 2017, 2019; however there are arguments that all black hole binaries may be considered as microquasars such as in Zhang 2013). Since  $\gamma$ -ray emission is theoretically expected to arise from microquasars (e.g., Atoyan & Aharonian 1999; Georganopoulos et al. 2002; Romero et al. 2003) and observationally the microquasars Cyg X-3 and Cyg X-1 were detected at  $\gamma$ -rays (Fermi LAT Collaboration et al. 2009; Tavani et al. 2009; Sabatini et al. 2010; Bodaghee et al.

2013; Malyshev et al. 2013), search for  $\gamma$ -ray emission from V404 Cygni was carried out. Loh et al. (2016) reported possible detection of the source ( $\sim 4.5\sigma$ ) in a 12-h time bin on 2015 Jun. 26 during the second outburst, where the data were obtained with the Large Area Telescope (LAT) onboard the *Fermi Gamma Ray Space Telescope (Fermi)*. The detection was seemingly confirmed by the *AGILE* observation, as Piano et al. (2017) reported their detection of the source near the same time in the energy range of 50–400 MeV (although the detection significance was  $\sim 4.3\sigma$ ). In addition, very-high-energy  $\gamma$ -ray observations were also conducted by the MAGIC telescopes in 2015 Jun., but no detection was found in the energy range of 200–1250 GeV (Ahnen et al. 2017).

Given that *Fermi* LAT has been collecting data for nearly 12 years and the database and source catalog were updated several times since the previous work by Loh et al. (2016), it is necessary to re-analyze the  $\gamma$ -ray data for V404 Cygni for the purpose of confirming the previous detection results and searching for new detection. We thus conducted detailed analysis. Different results were obtained. In this paper, we report the results.

## 2. LAT DATA ANALYSIS AND RESULTS

### 2.1. LAT data and source model

LAT has been scanning the whole sky continuously and collecting data in GeV band since 2008 Aug. (Atwood et al. 2009). We selected 0.1–500 GeV LAT events inside a  $20^\circ \times 20^\circ$  region (region of interest; RoI) centered at the position of V404 Cygni, over the time period from 2008-08-04 15:43:36 (UTC) to 2020-03-05 01:16:35 (UTC; approximately 11.5 yrs). The latest *Fermi* Pass 8 database was used. Following the recommendations of the LAT team<sup>1</sup>, the events with quality flags of ‘bad’ and zenith angles larger than 90 degrees were excluded; the latter is to prevent the Earth’s limb contamination.

Based on the very recently released *Fermi* LAT 10-year source catalog (4FGL-DR2), we constructed a source model (for 4FGL, see Abdollahi et al. 2020). The sources listed in 4FGL-DR2 that are within a 20 degree radius circular region from V404 Cygni were included in the source model. Their spectral forms are provided in the catalog. In our analysis, the sources within 5 degrees from the target were set to have free spectral parameters, and for the other sources, their spectral parameters were fixed at the values given in the catalog. The back-

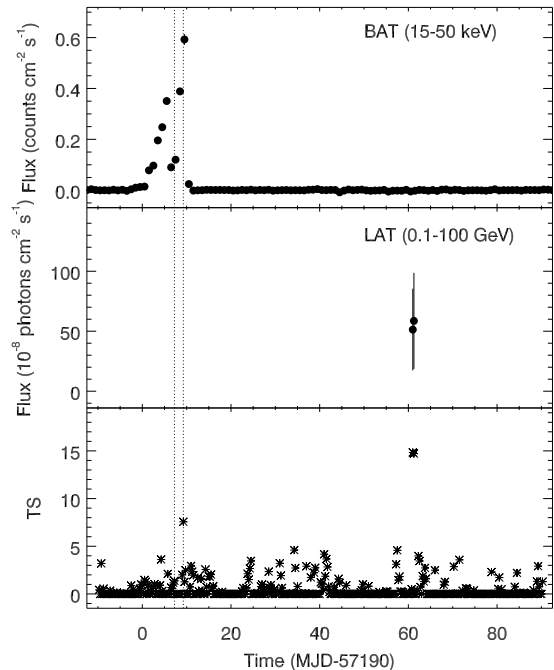


**Figure 1.** Smoothed TS curve (12-h bin with a 6-h shift) obtained for V404 Cygni in the energy range of 0.1–100 GeV (*bottom panel*). There are two TS points (at  $\sim$ MJD 57251) with values  $>9$ , whose fluxes are shown in the *middle panel*. To help indicate the outburst peak range, the *Swift* BAT hard X-ray light curve is shown in the *top panel*. The two dotted lines mark the time period of MJD 57197.25–57199.25, during which Loh et al. (2016) and Piano et al. (2017) reported possible detection of the source with *Fermi* LAT and *AGILE* respectively.

ground Galactic and extragalactic diffuse spectral models (glliem.v07.fits and iso.P8R3\_SOURCE\_V2.v1.txt respectively) were also included in the source model. Their normalizations were set as free parameters.

### 2.2. 2015 outburst

Since both *Fermi* LAT and *AGILE* possibly detected V404 Cygni during its 2015 outburst near Jun. 26 (MJD 57199; Piano et al. 2017), we repeated the analysis given in Loh et al. (2016). Standard binned likelihood analysis to the 0.1–100 GeV LAT data in each 12-h bins during the outburst were performed, where each time bin was shifted by 6 h forward (instead of 12 h) when constructing the time bins. Emission at the source position was assumed to have a power law. Since the outburst approximately ended during 2015 mid Aug. (Sivakoff et al. 2015), we extended the analysis to Aug. (compared to Jul. 17 as the end of data in Loh et al. 2016; see also their Figure 1). The obtained Test Statistic (TS) values were shown in Figure 1. There is a relatively high TS point at MJD 57199, but the value is  $<9$  (i.e., the de-

<sup>1</sup> <http://fermi.gsfc.nasa.gov/ssc/data/analysis/scitools/>

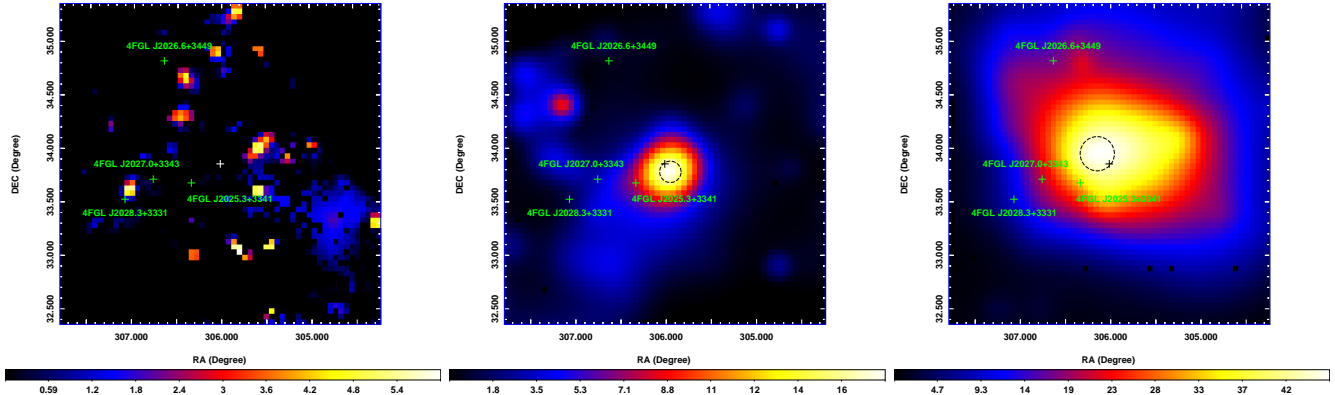


**Figure 2.** TS maps of the  $3^\circ \times 3^\circ$  region centered at V404 Cygni in the energy range of 0.3–500 GeV from the data of the whole time period (*left panel*), MJD 57251–57253 (*middle panel*), and MJD 57623–57625 (*right panel*). The image scale of the maps is  $0.05 \text{ pixel}^{-1}$ . The green pluses mark the catalog sources that were considered and removed in our analysis, and the white or black pluses mark the position of V404 Cygni. The dashed circle in each of the *middle* and *right* panels indicates the  $1\sigma$  error circle determined for the excess  $\gamma$ -ray emission.

tection significance is  $<3\sigma$ ), not as high as that given in Loh et al. (2016). Instead, we found two  $\text{TS} \sim 15$  points at MJD 57251 and 57251.25 (Aug. 17). Therefore based on our analysis to the Pass 8 data with the latest source catalog used, the claimed detection of V404 Cygni is questionable. For the data point at MJD 57251, we presented detailed analysis and results in the following Section 2.4.

### 2.3. Search for possible detection in the LAT time period

We analyzed the 11.5 yr LAT data to search for possible  $\gamma$ -ray emission from V404 Cygni. We first performed the binned likelihood analysis to the whole selected LAT data. The energy range of 0.3–500 GeV was used given the relatively large uncertainties of the instrument response function of LAT in the  $<0.3$  GeV energy range. Also in the low energy range, there is strong background emission or possible contamination from nearby sources for the regions along the Galactic plane (Galactic latitude of V404 Cygni is  $-2^\circ$ ). No emission was found at the position of the source from the analysis, as the obtained  $\text{TS} \sim 0$  (see the left panel of Figure 2).

Given that both microquasars Cyg X-3 and Cyg X-1 show variable  $\gamma$ -ray emission (e.g., Corbel et al. 2012; Bodaghee et al. 2013) and were significantly detected in short time periods such as in one-day time bins (e.g., Sabatini et al. 2010; Zdziarski et al. 2018), we focused on searching for detection in different short time bins from the likelihood analysis. We tested different time bins, such as 1-day, 3-day, or 6.5-day (i.e., the orbital period of V404 Cygni; Casares & Charles 1994) and found that the analysis to the data in 3-day time bins (Fig-

ure 3) well show possible detection over the LAT data time period.

First there were two  $\sim 440$  day time periods containing several points with  $\text{TS} > 9$  (marked as 1 and 2 respectively in Figure 3). When we changed to use 1-day or 6.5-day bins, no significantly better results were obtained for the data points in the two time periods. We tested to perform the likelihood analysis to the LAT data in each of the two  $\sim 440$  time periods, but the TS values were still low ( $\sim 3$ ). As  $\gamma$ -ray emission from a microquasar may be orbitally modulated (Fermi LAT Collaboration et al. 2009; Zdziarski et al. 2017), we also tested to divide the data in each time period into four orbital phase ranges, centered at phase 0.0, 0.25, 0.5, and 0.75, where the orbital parameters of V404 Cygni given by Casares & Charles (1994) were used. The TS results from the likelihood analysis indicated no detection in any of the orbital phase ranges. We concluded that no detection was found in the data of these two time periods.

However there are two 3-day bin data points with  $\text{TS} > 16$ , for which we mark with point 3 and 4 in Figure 3. The first is contained in the above time period 2 and was from the data in MJD 57251–57253. It is at the end of the 2015 outburst and was found to have  $\text{TS} \sim 15$  in our 12-h bin analysis (Figure 1). The second was from the data in MJD 57623–57625 and is more significant given  $\text{TS} \sim 45$ . Therefore we conducted detailed analysis for these two data points, which are given in the following sections.

### 2.4. Possible detection in MJD 57251–57253

In order to confirm this possible detection, we calculated a TS map of a  $3^\circ \times 3^\circ$  region centered at the

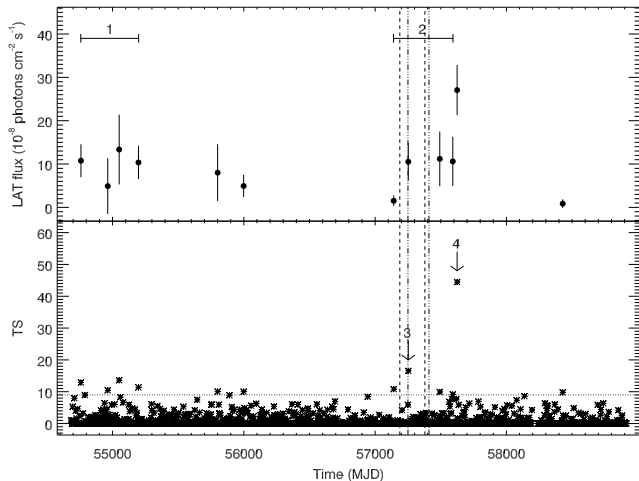


**Figure 3.** 3-day bin TS values (*bottom panel*) obtained at the position of V404 Cygni. For the  $TS > 9$  bins, the fluxes are shown in the *upper panel*. Two  $\sim 440$  day time periods (1 and 2) and two data points (3 and 4) are marked based on the TS values. The time periods of the 2015 outburst and mini-outburst are marked by the dashed (start time) and dash-dotted (end time) lines.

position of V404 Cygni. The obtained TS map is shown in the middle panel of Figure 2. Excess emission at the position of our target is clearly seen, with the maximum  $TS \approx 17.7$ . There are four catalog sources in the region. We note that although their positions are close to V404 Cygni, they caused negligible contamination to our analysis. Firstly the time period is short, only 3 days, and secondly these sources were not bright. For example the detection significances given in 4FGL-DR2 for the two closest sources are  $16\sigma$  and  $5\sigma$ . (Even we kept the sources when calculating the TS map, there were no notable changes to the obtained TS map.) We ran *gtfindsrc* in *Fermitools* to determine the position of the excess emission. The resulting  $1\sigma$  nominal uncertainty is  $0^\circ.1$ , and V404 Cygni is within the error circle (see Figure 2). We performed the likelihood analysis to the data with the fitted position and obtained a photon index of  $\Gamma = 2.5 \pm 0.4$  and a 0.3–500 GeV flux of  $F_{0.3-500} = 1.1 \pm 0.4 \times 10^{-7}$  photons  $s^{-1} cm^{-2}$  (with a TS value of 18).

The  $\gamma$ -ray spectrum of the excess emission was extracted by performing maximum likelihood analysis of the LAT data in 10 evenly divided energy bands in logarithm from 0.1–500 GeV. The spectral normalizations of the sources within 5 degrees from it were set as free parameters, while all the other parameters of the sources in RoI were fixed at the values obtained from the above maximum likelihood analysis. For the obtained spectral data points, we kept those when TS is greater than 4 and derived 95% flux upper limits otherwise. The re-

sults are provided in Table 1 and also shown in Figure 4. We note that there are only two data points with  $TS \geq 4$  at 0.2–0.5 GeV and 1.3–3.0 GeV respectively, and the second is more significant with  $TS \approx 20$ .

### 2.5. Detection in MJD 57623–57625

We performed the same analysis to the data in this 3-day bin as the above in Section 2.4. The TS map of the  $3^\circ \times 3^\circ$  region is shown in the right panel of Figure 2, indicating the maximum  $TS \approx 46.6$  at the target’s position. The determined position for the excess emission has a nominal uncertainty of  $0^\circ.16$ , and V404 Cygni is in the error circle. The likelihood analysis gave  $\Gamma = 2.9 \pm 0.3$  and  $F_{0.3-500} = 2.7 \pm 0.6 \times 10^{-7}$  photons  $s^{-1} cm^{-2}$  (with a TS value of 47). The  $\gamma$ -ray spectrum was obtained, with the results given in Table 1 and shown in Figure 4. The emission is still soft, mostly detected in the energy range of 0.1–1.3 GeV.

Since the excess emission has relatively high TS value, we constructed a short time-bin light curve around the detection. To avoid the large uncertainties in the low energy end, we used the data in the 0.3–500 GeV energy range. We found that a one-day light curve, shifted forward by 0.25 day, may reveal the detailed variations. As shown in Figure 5, the source appears to have a sudden brightening and then a relatively slow decay. Using the orbital parameters given in Casares & Charles (1994), we checked the orbital phases for the time period. The start and end times (MJD 57623.0 and 57626.0 respectively) correspond to the orbital phase 0.32 and 0.78 respectively (when the companion star was mostly behind the black hole).

## 3. DISCUSSION

Having used the latest *Fermi* LAT database and source catalog, we re-analyzed the LAT data for searching for possible detection of V404 Cygni at  $\gamma$ -rays. Different from that reported in Loh et al. (2016), we did not find similar possible detection near the peak of the 2015 outburst (or possible detection in its mini-outburst). Instead, we found one possible detection ( $\sim 4\sigma$ ) at the end of the outburst and one at the time period of MJD 57623–57626 with a significance of  $\sim 7\sigma$ . The excess emission in each detection matches V404 Cygni in position. Because the positional uncertainties are relatively large ( $0^\circ.1$  and  $0^\circ.16$ ), we checked the SIMBAD Astronomical Database for sources within the  $0^\circ.16$  error circle. There are only several galaxies, detected by *NuSTAR* at the hard X-ray range of 3–24 keV and identified at optical and infrared wavelengths (Lansbury et al. 2017), within the error circle, and no blazars, which are the dominant  $\gamma$ -ray sources in the sky (Abdollahi et al. 2020).

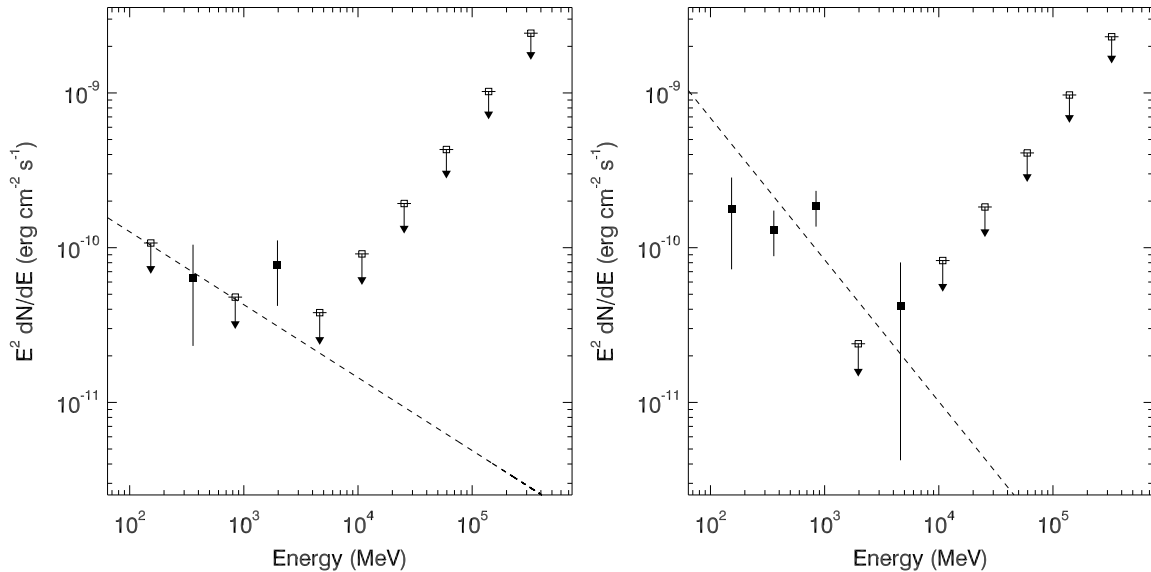


**Figure 4.**  $\gamma$ -ray spectra of the excess emission determined in MJD 57251–57253 (*left* panel) and MJD 57623–57625 (*right* panel). The black squares are the spectral data points with  $\text{TS} \geq 4$ , and the open squares are the 95% flux upper limits. The model fits obtained from the likelihood analysis are shown as the dashed lines respectively in the two panels.

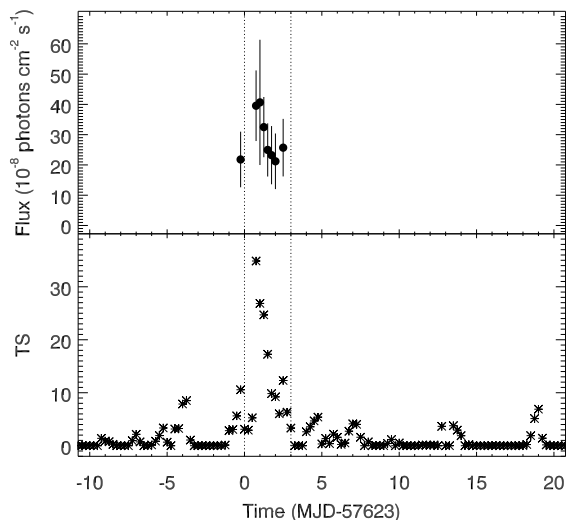


**Figure 5.** Fluxes and TS values in one-day bins (*top* and *bottom* panel respectively), shifted forward by 0.25 day, around the MJD 57623–57625 detection. Only fluxes with  $\text{TS} \geq 9$  are shown. The two dotted lines indicate the time period of MJD 57623–57625.

The excess emission at the position of V404 Cygni is soft. For the latter detection with sufficiently high significance,  $\Gamma = 2.9 \pm 0.3$  and the dominant emission is in the energy range of  $\leq 1.3$  GeV. This emission is similar to that observed in the flaring events of Cyg X-3 and Cyg X-1 (Fermi LAT Collaboration et al. 2009; Zdziarski et al. 2018, 2017). In addition,  $\gamma$ -ray emission is seen at spots in the lobes of the jets from the microquasar SS 433 (Abeysekara et al. 2018; Xing et al. 2019). Although the origin of the GeV  $\gamma$ -ray emission is under

discussion (e.g., Rasul et al. 2019; Sun et al. 2019), it is extremely soft with  $\Gamma \sim 6$  and in the energy range of  $\leq 1.8$  GeV (Xing et al. 2019). These similarities support the association of the excess emission with V404 Cygni. In case that the detection was due to a flare from an unseen background blazar, we checked the properties of the identified blazars in the LAT source catalog. Most of them have emission much harder than the excess emission. For example, one of 1190 BL Lac type and 24 of 730 flat-spectrum-radio-quasar type blazars have  $\Gamma \geq 2.9$ . It is very unlikely to have a blazar in a random  $0^\circ.16$ -radius circular region only showing a three-day, soft-emission flare.

Based on the likelihood analysis results for the MJD 57623–57625 detection, the observed 0.3–500 GeV (isotropic) luminosity is  $\sim 1.9 \times 10^{35}$  erg s $^{-1}$ . The jet luminosity (collimation corrected; see Lamb et al. 2017) from V404 Cygni could be a factor of  $\sim 20$  larger, that is  $\sim 4 \times 10^{36}$  erg s $^{-1}$ . From fitting the optical and infrared broad-band spectrum of the source, the mass accretion rate was estimated to be  $\sim 7 \times 10^{16}$  g s $^{-1}$  (Muno & Mauerhan 2006), indicating an accretion power of  $\sim 6 \times 10^{37} \eta$  erg s $^{-1}$  (where  $\eta$  is the efficiency) in the binary system. Therefore there is sufficient energy to power such jet emission even in quiescence. Given these considerations, i.e., the match in position, the soft spectrum similar to those of the  $\gamma$ -ray microquasars, and sufficient accretion power, we conclude that we have detected V404 Cygni likely during MJD 57623–57625 and possibly during MJD 57251–57253.

Different models with jets considered have been proposed to explain  $\gamma$ -ray emission from microquasars (e.g., Atoyan & Aharonian 1999; Georganopoulos et al. 2002; Romero et al. 2003). Based on detailed studies of Cyg X-1 (also Cyg X-3; see, e.g., Zdziarski et al. 2018), which are able to fit its broad-band spectrum from radio to  $\gamma$ -rays, the  $\gamma$ -ray emission is determined to likely contain the components due to jets' synchrotron self-Compton radiation and upscattering of photons from the accretion disk and companion star (Zdziarski et al. 2014, 2017).  $\gamma$ -ray flares are due to jet activity, clearly shown in the case of Cyg X-3 from radio and  $\gamma$ -ray monitoring (Corbel et al. 2012). For V404 Cygni in the quiescent state, radio observations have shown both significant long-term and short-term flux variations, in the latter of which the flares were seen to exhibit a possible pattern of having fast rise and slow decay (Plotkin et al. 2019). We note that the detection in MJD 57623–57625 shows a possibly similar pattern (Figure 5), although its time scale is much longer than hour-long time scales observed at radio frequencies. There were a few radio observations of V404 Cygni in quiescence (Plotkin et al. 2019), but none of them were conducted at times very close to the two  $\gamma$ -ray events we have found. Hopefully a close radio monitoring of the source over a long term may be possible in the near future with more advanced radio facilities, which may help reveal the connection between radio and  $\gamma$ -ray flares. We checked the *Swift* BAT data (Krimm et al. 2013), but did not find any significant brightening around the LAT detection in the daily 15–50 keV light curve of V404 Cygni.

This detection of the  $\gamma$ -ray flaring events from V404 Cygni in its quiescent state establishes the source as another microquasar with detectable  $\gamma$ -ray emission, and moreover exhibits interesting features among  $\gamma$ -ray microquasars. For example, no detection was found during the outburst or mini-outburst when jet ejection was ob-

served at radio and millimeter frequencies or indirectly derived from X-ray observations (Tetarenko et al. 2017, 2019; Walton et al. 2017). If the detection at the end of the outburst was true, it might provide a hint to the physical process, any particular jet activity, at that end phase. In order to understand how high-energy emission is related to jet activity in such a case, simultaneous  $\gamma$ -ray and radio detection will provide key information. However it is not easy to obtain such detection since based on our search, detectable  $\gamma$ -ray flaring events from V404 Cygni are rare. Finally, different from Cyg X-3 and Cyg X-1 (note that SS 433 is a peculiar case; Abeysekara et al. 2018) that have a high-mass companion, this binary belongs to the more-general low-mass X-ray binary (LMXB) class. We thus may consider that LMXBs with jets (including neutron star LMXBs; e.g., Russell et al. 2006) might all be able to produce some sorts of  $\gamma$ -ray emission, and searches for short-term flaring events among them might produce interesting results.

#### ACKNOWLEDGMENTS

We thank F. Xie for useful discussion about jet activity in different black-hole X-ray binaries. This research made use of the High Performance Computing Resource in the Core Facility for Advanced Research Computing at Shanghai Astronomical Observatory. This research was supported by the National Program on Key Research and Development Project (Grant No. 2016YFA0400804) and the National Natural Science Foundation of China (11633007, U1738131). Z.W. acknowledges the support by the Original Innovation Program of the Chinese Academy of Sciences (E085021002).

#### REFERENCES

- Abdollahi, S., Acero, F., Ackermann, M., et al. 2020, *ApJS*, 247, 33
- Abeysekara, A. U., Albert, A., Alfaro, R., et al. 2018, *Nature*, 562, 82
- Ahnen, M. L., Ansoldi, S., Antonelli, L. A., et al. 2017, *MNRAS*, 471, 1688
- Atoyan, A. M., & Aharonian, F. A. 1999, *MNRAS*, 302, 253
- Atwood, W. B., Abdo, A. A., Ackermann, M., et al. 2009, *ApJ*, 697, 1071
- Barthelmy, S. D., D’Ai, A., D’Avanzo, P., et al. 2015, *GRB Coordinates Network*, 17929, 1
- Belloni, T. M., & Motta, S. E. 2016, *Astrophysics and Space Science Library*, Vol. 440, *Transient Black Hole Binaries*, 61
- Bodaghee, A., Tomsick, J. A., Pottschmidt, K., et al. 2013, *ApJ*, 775, 98
- Casares, J., & Charles, P. A. 1994, *MNRAS*, 271, L5
- Casares, J., Charles, P. A., & Naylor, T. 1992, *Nature*, 355, 614
- Corbel, S., Dubus, G., Tomsick, J. A., et al. 2012, *MNRAS*, 421, 2947
- Fermi LAT Collaboration, Abdo, A. A., Ackermann, M., et al. 2009, *Science*, 326, 1512

- Gallo, E., Fender, R. P., & Hynes, R. I. 2005, *MNRAS*, 356, 1017
- Georganopoulos, M., Aharonian, F. A., & Kirk, J. G. 2002, *A&A*, 388, L25
- Khargharia, J., Froning, C. S., & Robinson, E. L. 2010, *ApJ*, 716, 1105
- Krimm, H. A., Holland, S. T., Corbet, R. H. D., et al. 2013, *ApJS*, 209, 14
- Lamb, G. P., Kobayashi, S., & Pian, E. 2017, *MNRAS*, 472, 475
- Lansbury, G. B., Stern, D., Aird, J., et al. 2017, *ApJ*, 836, 99
- Loh, A., Corbel, S., Dubus, G., et al. 2016, *MNRAS*, 462, L111
- Maitra, D., Scarpaci, J. F., Grinberg, V., et al. 2017, *ApJ*, 851, 148
- Makino, F. 1989, *IAUC*, 4782, 1
- Malyshev, D., Zdziarski, A. A., & Chernyakova, M. 2013, *MNRAS*, 434, 2380
- Miller-Jones, J. C. A., Jonker, P. G., Dhawan, V., et al. 2009, *ApJL*, 706, L230
- Mirabel, I. F., & Rodríguez, L. F. 1999, *ARA&A*, 37, 409
- Muñoz-Darias, T., Casares, J., Mata Sánchez, D., et al. 2017, *MNRAS*, 465, L124
- Muno, M. P., & Mauerhan, J. 2006, *ApJL*, 648, L135
- Piano, G., Munar-Adrover, P., Verrecchia, F., Tavani, M., & Trushkin, S. A. 2017, *ApJ*, 839, 84
- Plotkin, R. M., Miller-Jones, J. C. A., Chomiuk, L., et al. 2019, *ApJ*, 874, 13
- Plotkin, R. M., Miller-Jones, J. C. A., Gallo, E., et al. 2017, *ApJ*, 834, 104
- Rana, V., Loh, A., Corbel, S., et al. 2016, *ApJ*, 821, 103
- Rasul, K., Chadwick, P. M., Graham, J. A., & Brown, A. M. 2019, *MNRAS*, 485, 2970
- Rodríguez, J., Cadolle Bel, M., Alfonso-Garzón, J., et al. 2015, *A&A*, 581, L9
- Romero, G. E., Torres, D. F., Kaufman Bernadó, M. M., & Mirabel, I. F. 2003, *A&A*, 410, L1
- Russell, D. M., Fender, R. P., Hynes, R. I., et al. 2006, *MNRAS*, 371, 1334
- Sabatini, S., Tavani, M., Striani, E., et al. 2010, *ApJL*, 712, L10
- Sivakoff, G. R., Bahramian, A., Altamirano, D., et al. 2015, *The Astronomer's Telegram*, 7959, 1
- Sun, X.-N., Yang, R.-Z., Liu, B., Xi, S.-Q., & Wang, X.-Y. 2019, *A&A*, 626, A113
- Tavani, M., Bulgarelli, A., Piano, G., et al. 2009, *Nature*, 462, 620
- Tetarenko, A. J., Sivakoff, G. R., Miller-Jones, J. C. A., et al. 2017, *MNRAS*, 469, 3141
- . 2019, *MNRAS*, 482, 2950
- Walton, D. J., Mooley, K., King, A. L., et al. 2017, *ApJ*, 839, 110
- Xing, Y., Wang, Z., Zhang, X., Chen, Y., & Jithesh, V. 2019, *ApJ*, 872, 25
- Zdziarski, A. A., Malyshev, D., Chernyakova, M., & Pooley, G. G. 2017, *MNRAS*, 471, 3657
- Zdziarski, A. A., Pjanka, P., Sikora, M., & Stawarz, L. 2014, *MNRAS*, 442, 3243
- Zdziarski, A. A., Malyshev, D., Dubus, G., et al. 2018, *MNRAS*, 479, 4399
- Zhang, S.-N. 2013, *Frontiers of Physics*, 8, 630

**Table 1.** Flux measurements for V404 Cygni from two sets of 3-day LAT data

$E$ (GeV)	Band (GeV)	MJD 57251–57253		MJD 57623–57625	
		$F/10^{-10}$ (erg cm $^{-2}$ s $^{-1}$ )	TS	$F/10^{-10}$ (erg cm $^{-2}$ s $^{-1}$ )	TS
0.15	0.1–0.2	1.1	0	2±1	12
0.36	0.2–0.5	0.6±0.4	4	1.3±0.4	14
0.84	0.5–1.3	0.5	0	1.8±0.5	44
1.97	1.3–3.0	0.8±0.3	20	0.2	0
4.62	3.0–7.1	0.4	0	0.4±0.3	5
10.83	7.1–16.6	0.9	0	0.8	0
25.37	16.6–38.8	1.9	0	1.8	0
59.46	38.8–91.0	4.3	0	4.1	0
139.36	91.0–213.3	10.2	0	9.7	0
326.60	213.3–500.0	24.3	0	23.1	0

Note:  $F$  is the energy flux ( $E^2 dN/dE$ ), and fluxes without un certainties are 95% upper limits.